

Step-recovery diode phase-standard characterisation and preliminary structure-based covariance compression algorithm

David Humphreys, Peter Harris, Matthew Harper,
James Miall
Electromagnetic Technologies
National Physical Laboratory
Teddington, UK
matthew.harper@npl.co.uk

Dominique Schreurs
Katholieke Universiteit Leuven
B-3001 Leuven, België
dominique.schreurs@esat.kuleuven.be

Abstract— The traceability route for phase-standards is outlined together with a preliminary compression algorithm that allows the uncertainties, represented as a covariance matrix, to be efficiently stored so that they may be represented in either the time or frequency domains. The final algorithm will be available on the Euramet IND016 website.

Comb generators, uncertainties, covariance matrix, nonlinear measurements, sampling oscilloscope, phase measurements.

I. INTRODUCTION

Characterisation of the non-linear behaviour of devices under large-signal conditions requires the simultaneous measurement of forward and reverse travelling voltage-wave signals at multiple frequencies, often, but not always, in a system with 50Ω impedance. The accuracy of the results will depend on a time reference, which can be realised as a calibrated receiver, typically a sampling gate or a Digital Sampling Oscilloscope (DSO), or by using a source that generates phase-locked harmonic signals, such as a comb generator (mixer-based solutions). The different system architectures to realise nonlinear measurements use one or other of these approaches, as outlined in Fig. 1.

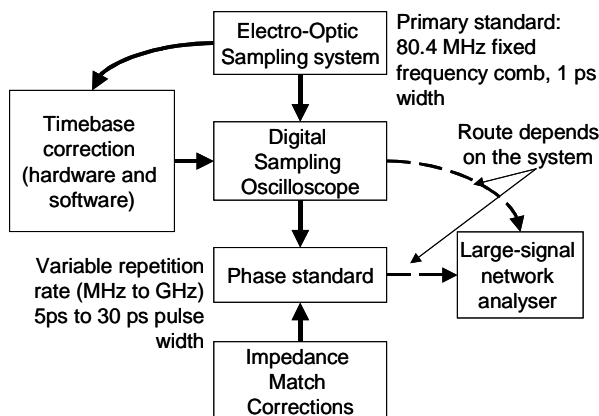


Figure 1. Traceability routes at NPL for Large-Signal Network Analysers

Two industrial drivers are:

1. To improve the phase standard (PS) phase accuracy traceable to national standards. A typical target accuracy would be two degrees over the operating range,
2. To increase the density of the comb-harmonics, to ensure maximum coverage in the frequency domain (lowering the pulse repetition rate).

The national measurement institute drivers are:

1. To ensure a traceable and reproducible approach,
2. To provide a useable representation of the confidence interval in both the time and frequency domains.

In previous work we identified measurement and modelling strategies to achieve a traceable and reproducible approach for the current PS technologies [1] building on previous work carried out at NIST [2]. Measurement uncertainties of a waveform in the time or frequency domain show structure that can be captured using a covariance matrix approach [3]. This provides a representation that can be readily expressed in either the time domain or the frequency domain. The frequency-domain covariance matrix is formulated in terms of the real and imaginary components so that all the correlation relationships are maintained. The issue is that covariance matrix grows as the square of the number of trace elements (n^2). The aim of this work has been to develop an approach that provides an adequate representation of the uncertainties but grows at a lower rate (n) [4].

II. TRACEABILITY PATH FOR HARMONIC PHASE AND PHASE STANDARDS

Within NPL [5] and other national standards laboratories (NIST [6] and PTB [7]) the primary standard for dynamic electrical measurements is realised through electro-optic sampling using the Pockels effect, where the polarisation of the light passing through an electro-optic crystal, such as Lithium Tantalate (LiTaO_3), is rotated in the presence of an electrical field. The NPL Electro-Optic Sampling system (EOS) splits the output pulses from a modelocked Ti:sapphire laser (sub-200 fs full-width at half-maximum (FWHM) at a repetition rate of 80.4 MHz; lower pulse repetition rates can be achieved by gating the output). Part of the split output drives a fast

photoconductor to generate a comb of electrical pulses (approximately 1 ps FWHM) on a coplanar waveguide (CPW) transmission-line. The remainder is used, with an adjustable delay, to probe the electric field above the CPW line and to determine the cross-correlation waveform. The Pockels effect is fast (10^{-15} s) giving an EOS bandwidth of about 800 GHz on the CPW line. In practice, the maximum usable frequency is lower (in the region of 100 – 200 GHz) due to the transition from coplanar to coaxial geometry and corrections for mismatch.

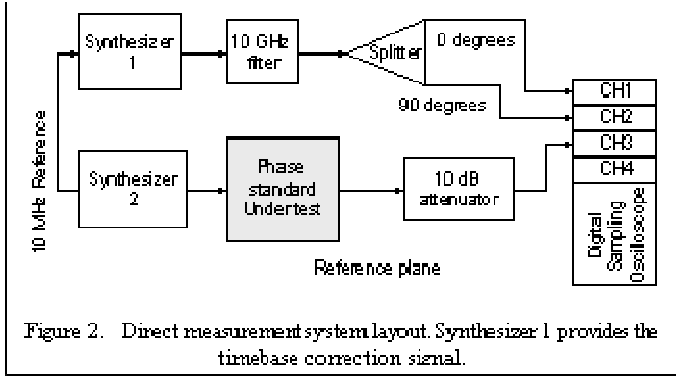


Figure 2. Direct measurement system layout. Synthesizer 1 provides the timebase correction signal.

The CPW line is only 500 – 2000 μm long to avoid dispersion. A coplanar-to-coaxial transition provides the comb output pulses in the correct geometry for connection to the DSO under calibration. The coplanar-to-coaxial transition is characterised using the EOS system. The maximum delay that can be realized through the translation stage is 13 ns with a minimum point spacing of 9 fs. In practice the measured epoch

$$\dots \tag{1}$$

is typically 500 – 2000 ps with 0.25 ps resolution. The frequency data available from this system is sparse in comparison to the comb generators.

III. DEVICES AND MEASUREMENT SYSTEM

A. Phase standard

In this work we have used the results for a step-recovery diode based PS that is specified to operate over an octave bandwidth 600 MHz – 1200 MHz. The RF power-level is monitored using an external RF power meter to ensure a reproducible operating point.

B. Measurement systems

All the measurements have been taken using a single DSO using timebase correction which is essential to compensate for jitter and timebase nonlinearity [8], [9]. We use a separate synthesiser to generate the timebase reference signals. The frequency is chosen such that no intermodulation products arising from re-modulation of any comb line by the IQ frequency, or its harmonics, fall on any other comb lines. The synthesisers are locked using their 10 MHz reference signals.

The trigger signal for the DSO was obtained from the synthesiser or phase standard as appropriate. The residual jitter, which has several contributing factors, including the reference lock quality, was negligible (< 500 fs rms).

Measurements were taken at different comb frequencies using DSOs with 70 GHz bandwidth sampling heads and a 10 dB attenuator was included to give an input return loss better than 10 dB (see Fig. 2). The aim of these measurements is to minimise the errors by providing the best overall match.

IV. COVARIANCE MATRIX STRUCTURE AND FORMULATION

In this analysis, the uncertainties are linearized and represented by a Taylor series expansion, which can be represented as a covariance matrix. In principle, the covariance matrix can be formulated from the waveform results in either the time-domain or the frequency-domain. The reason for calculating the covariance matrix in the frequency domain is that the upper frequency limit is set and so extending the epoch can be achieved by interpolating the array. Also, timebase corrected DSO results are unevenly spaced and are transformed to the frequency domain by a least-squares Fourier fit. The covariance matrix is designed to maximise visibility of structural relationships by separating the results into their real and imaginary components,

Where the error term is given by,

$$\tag{2}$$

and is the measured response as a complex voltage. Removing redundant elements, the minimum uncompressed

storage requirement for the full matrix is

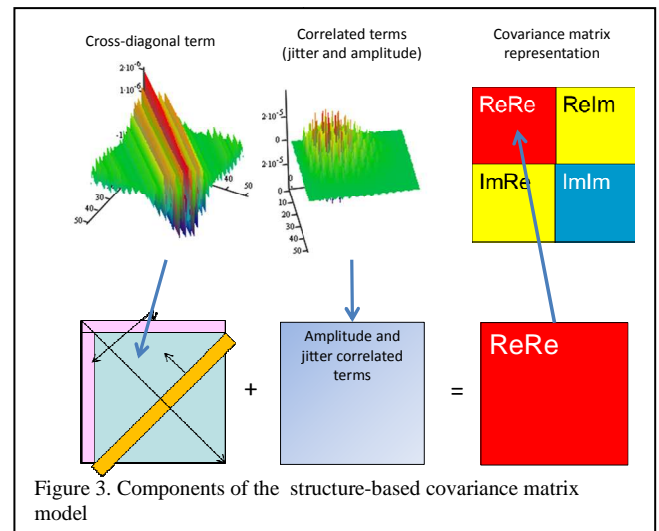


Figure 3. Components of the structure-based covariance matrix model

Treating the matrix as sparse and setting elements to zero can give savings but should be approached with caution [10].

By separating the covariance matrix into the $\langle \text{Re} \cdot \text{Re} \rangle$, $\langle \text{Im} \cdot \text{Im} \rangle$, and cross-terms the underlying structures are revealed. Each block in the covariance matrix structure shows both correlated and uncorrelated signal components. The uncorrelated terms that appear as cross-diagonal elements show some symmetry, allowing the response to be represented by a smaller number of terms, each of length n . The time-error (jitter) and amplitude variation components are highly correlated and can also be represented by single parameters, which can be recovered by a least-squares analysis. The first row and column of each block must be separately stored as these exhibit different characteristics from the remainder of the matrix. This is illustrated in Fig. 3.

V. MEASUREMENT RESULTS

The PS shows variation of the pulse shape with RF drive frequency and RF drive power, illustrated in Fig. 4. in the time-domain.

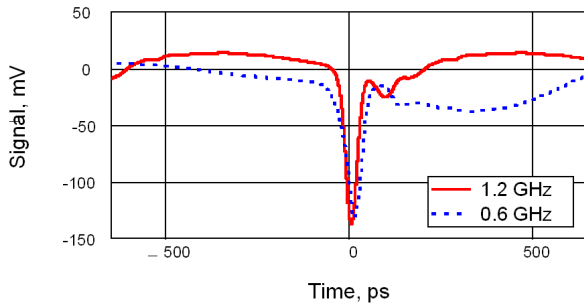


Figure 4. Variation of time-domain response with drive frequency

These results have not been corrected for residual jitter components. The covariance analysis has been applied at a single frequency only since the device is fully nonlinear with RF power and frequency.

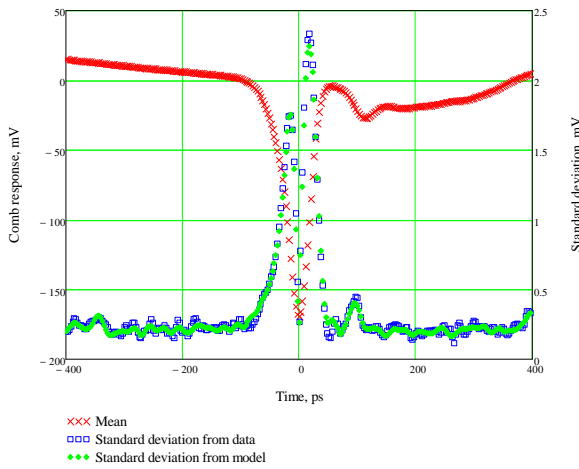


Figure 5. Time-domain response showing mean and standard deviation calculated from the measured and aligned data and from the model.

VI. VERIFICATION OF THE COVARIANCE MODEL USING MEASURED RESULTS

A measurement of an RF comb phase-standard operating at a repetition rate of 700 MHz has been used as a test example. The measurement was performed using a sampling oscilloscope and the time-domain response is shown in Fig. 5 together with the uncertainties calculated from the results and through the model. The measurement set comprises twenty traces of 4050 points. Each trace was corrected for jitter and timebase nonlinearity and the Fourier coefficients at the comb harmonics were calculated by least-squares fitting to give twenty data sets, which is insufficient to meet the decomposition criteria.

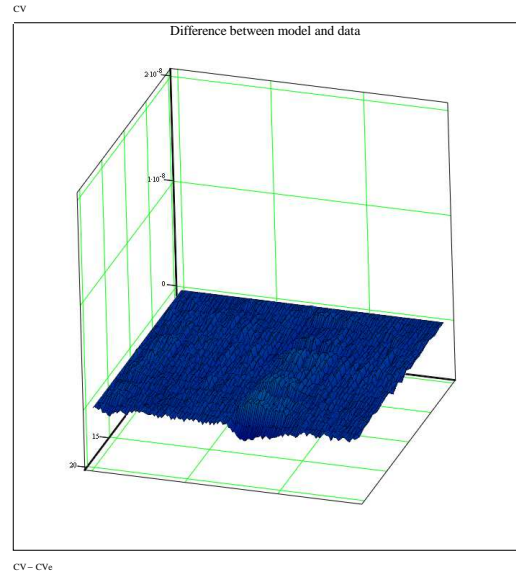
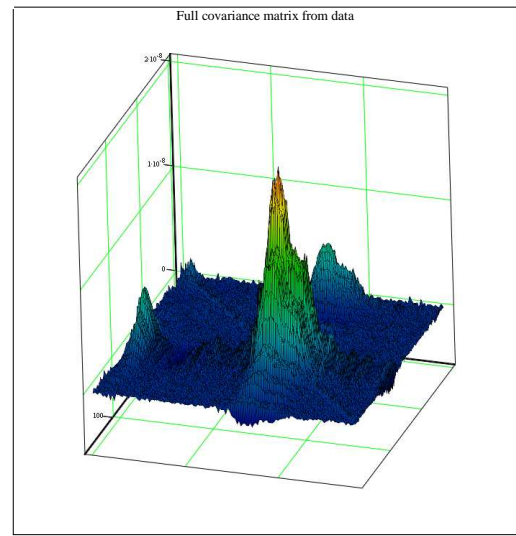
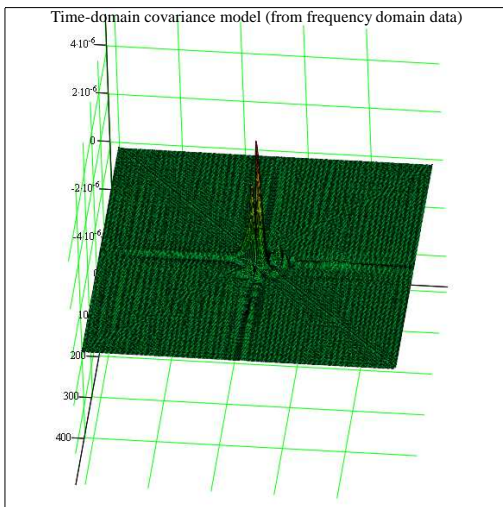
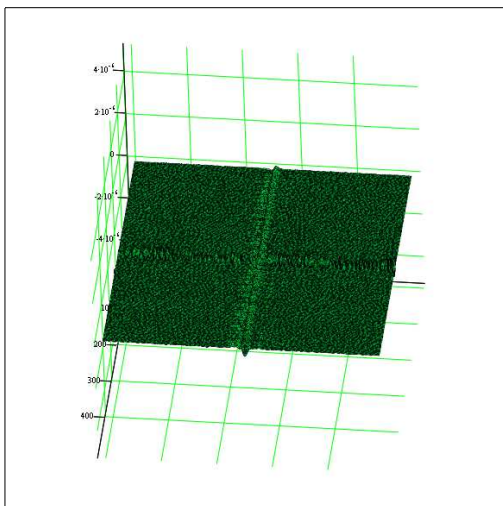


Figure 6. Frequency domain covariance and model fit showing the correlated components.

The covariance matrix in the frequency domain (Fig. 6) shows that there are significant correlated components, which accounts for the variation of the uncertainties with time.



CV_t



CV_t - CV_f

Figure 7. Frequency domain covariance and model fit showing the correlated components.

The frequency-domain covariance matrix has been converted into the time-domain, using the relationship,

$$CV_t = CV_f^T A \quad (2)$$

Where the matrix A contains the Fourier transform operator components. The time-domain results (Fig.7) also show correlated components and the difference between the transform of the model and the transform of the measured results is small.

VII. CONCLUSIONS

We have outlined the traceability route for comb-based phase standards and described a covariance matrix compression algorithm that reduces the storage requirements from $\frac{1}{2}n(n+1)$ to $10n$, where n is the number of frequency components. The data presented show a good fit and the results can be used in either the time or the frequency domain. This is the first step to allow waveform uncertainties to be stored and applied to measured results.

The measurement system uses a DSO traceably calibrated against the NPL primary standard and allows measurement of time epochs of 200 ns with a point spacing of 2 ps. Timebase correction is essential to achieve high accuracy.

This software has been developed as part of the Euramet IND016 project. The final version of the covariance compression algorithm will be available through the Euramet IND016 website [11].

ACKNOWLEDGMENT

The authors thank the Euramet project team for their help with this work.

REFERENCES

- [1] D. A. Humphreys, M. R. Harper, J. Miall, D. Schreurs, "Characterization and behavior of comb phase-standards," Microwave Conference (EuMC), 2011 41st European , vol., no., pp.926-929, 10-13 Oct. 2011.
- [2] H. C. Reader, D. F. Williams, P. D. Hale, and T. S. Clement, "Comb-Generator Characterization," IEEE Trans. MTT, vol 56 (2), pp 515-521, February 2008.
- [3] D. F. Williams, A. Lewandowski, T. S. Clement, C. M. Wang, P. D. Hale, J. M. Morgan, D. A. Keenan, and A. Dienstfrey, "Covariance-based uncertainty analysis of the NIST electro-optic sampling system," IEEE Trans. Microwave Theory Tech., vol. 54, no. 3, pp. 481-491, Jan. 2006.
- [4] D. A. Humphreys, P. M. Harris, J. Miall, "Instrument related structure in covariance matrices used for uncertainty propagation," Microwave Conference (EuMC), 2012 43rd European , 28 Oct.- 2 Nov. 2012.
- [5] M R Harper, A J A Smith, A Basu, and D A Humphreys. 2004. "Calibration of a 70 GHz Oscilloscope," CPEM 2004, London, June 27 to July 2, 2004: 530-531.
- [6] D. F. Williams, P. D. Hale, T. S. Clement, and J. M. Morgan, "Calibrated 200-GHz Waveform Measurement," IEEE Trans. MTT, vol 53 (4), pp. 1384-1389, April 2005.
- [7] M. Bieler, M. Spitzer, K. Pierz, and U. Siegner, "Improved Optoelectronic Technique for the Time-Domain Characterization of Sampling Oscilloscopes," IEEE Trans. Instrum. Meas. 58, 1065-1071 (2009).
- [8] D. A. Humphreys and F. Bernard, "Compensation of sampling oscilloscope trigger jitter by an in-phase and quadrature referencing technique," ARMMS Meeting Abingdon, UK, April 2005.
- [9] D A Humphreys, "Vector Measurement of Modulated RF Signals by an In-Phase and Quadrature Referencing Technique," IET Proc. Sci. Meas. Tech, BEMC Special edition, IEE vol. 153, no 6, pp. 210-216., Nov. 2006.
- [10] A. Jalobeanu, J. A. Gutiérrez, "Inverse covariance simplification for efficient uncertainty management," 27th International Workshop on Bayesian Inference and Maximum Entropy Methods in Science and Engineering, AIP Conf. Proc. 954, pp.237-244, July 2007.
- [11] . <http://www.ptb.de/emrp/235.html>